

## Supporting Information

Electrochromic Switching and Nanoscale Electrical Properties of a Poly(5-cyano indole)-Poly(3,4-ethylenedioxy pyrrole) Device with a Free Standing Ionic Liquid Electrolyte

Oxidation potentials of the monomers:

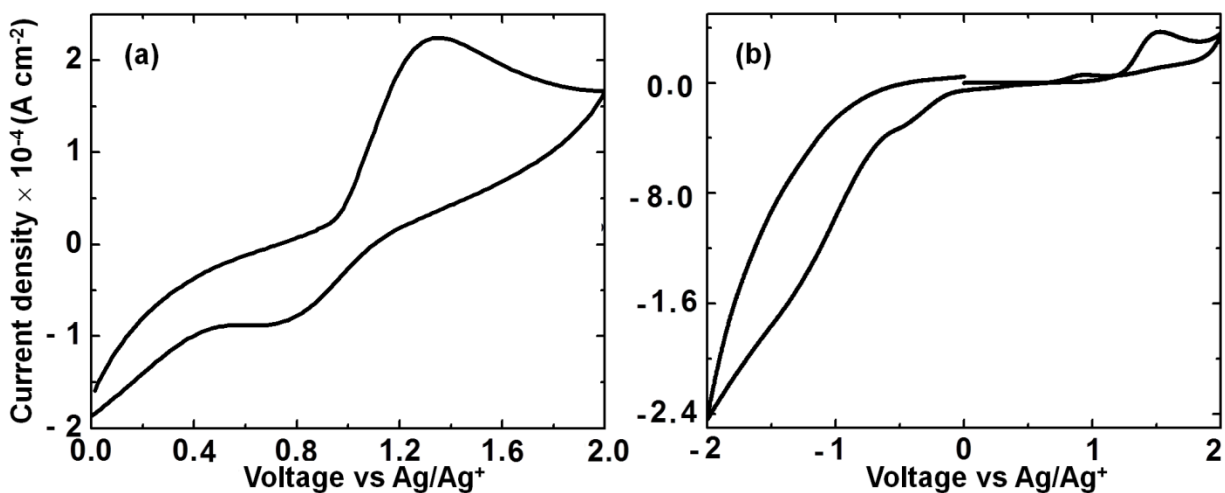


Figure S1 Cyclic voltammograms of the monomers: (a) 5-cyano indole and (b) 3,4-ethylenedioxy pyrrole) in the FAP ionic liquid: trihexyl(tetradecyl)phosphonium tris(pentafluoroethyl)trifluorophosphate or  $[(\text{C}_{32}\text{H}_{68})\text{P}^+][(\text{C}_2\text{F}_5)_3\text{PF}_3^-]$ , recorded at  $20 \text{ mV s}^{-1}$ , with Pt as counter electrode and Ag/AgCl/KCl as the reference electrode.

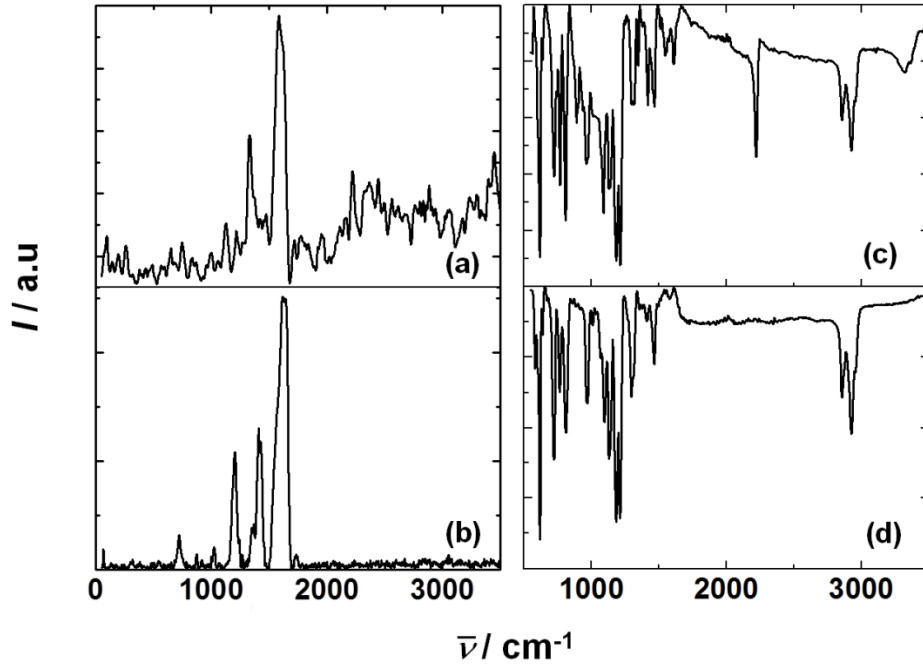


Figure S2 Raman spectra of (a) PCIND and (b) PEDOP films and FTIR spectra of (c) PCIND and (d) PEDOP films.

Table S1 FTIR and Raman band positions and assignments for PCIND and PEDOP films.

PCIND		PEDOP		Description
FTIR (cm <sup>-1</sup> )	Raman (cm <sup>-1</sup> )	FTIR (cm <sup>-1</sup> )	Raman (cm <sup>-1</sup> )	
2926	—	2925	—	$\nu(\text{C}=\text{C}-\text{H})$
2856	—	2856	—	$\nu(-\text{C}-\text{H})$
2220	—	—	—	$\nu(\text{C}\equiv\text{N})$
1609	1650	—	1578	$\nu(\text{C}=\text{C})$
1380	1355	1310	1355	$\nu(\text{C}_\beta-\text{C}_\beta)$
1212	1230	1210	1290	$\nu(\text{C}-\text{N})$
—	—	1066	—	$\delta(\text{C}-\text{O}-\text{C})$
888	845	862	872	$\nu(\text{P}-\text{F})$
766, 722	—	762, 719	—	$\delta(\text{C}-\text{N}-\text{C})$
—	720	—	720	$\delta(\text{N}-\text{H})$

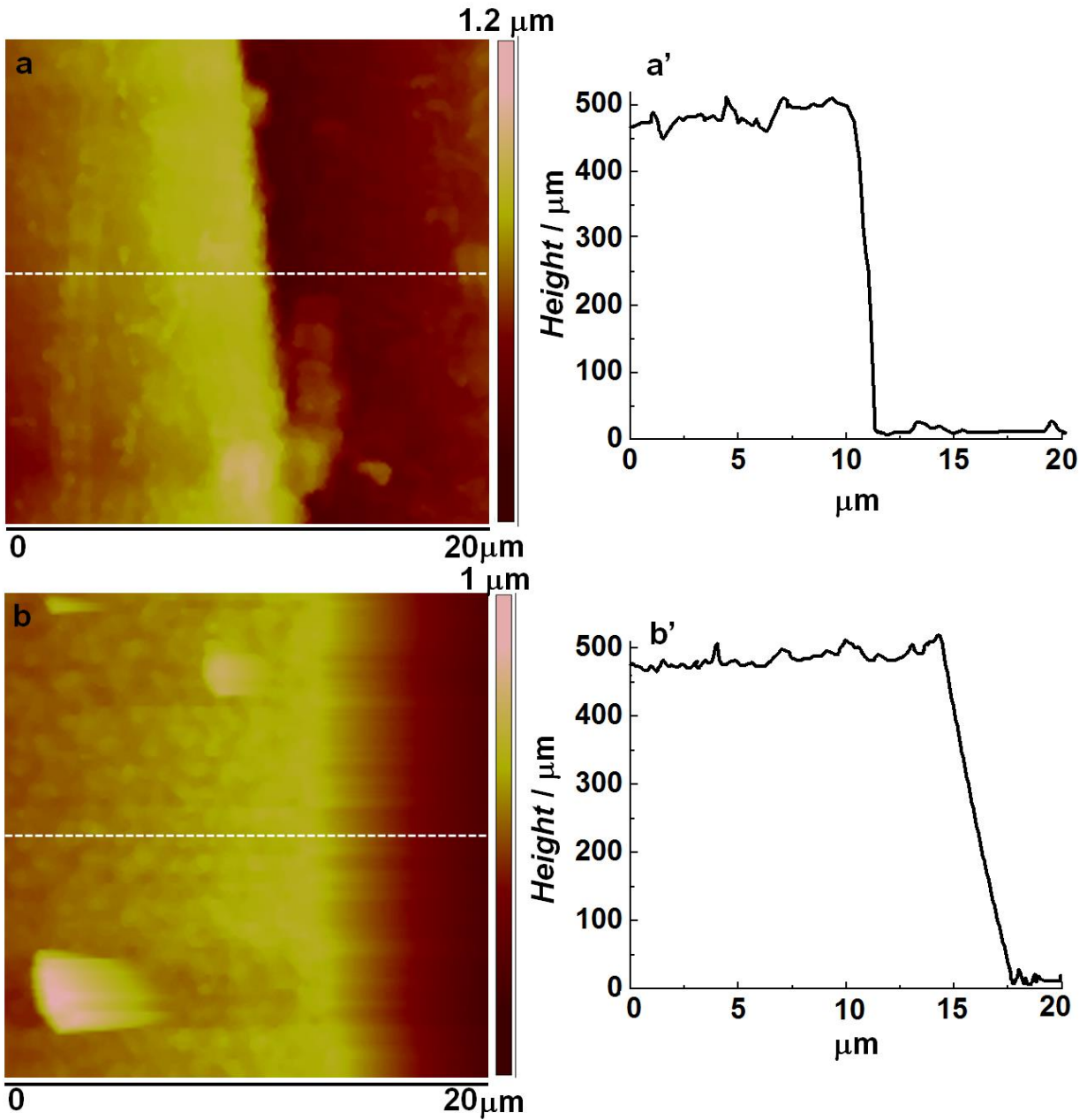


Figure S3 AFM images of (a) PCIND and (b) PEDOP films, (a') and (b') are the corresponding section profiles obtained along the dashed lines shown in (a) and (b). The step height corresponds to thickness of the film.

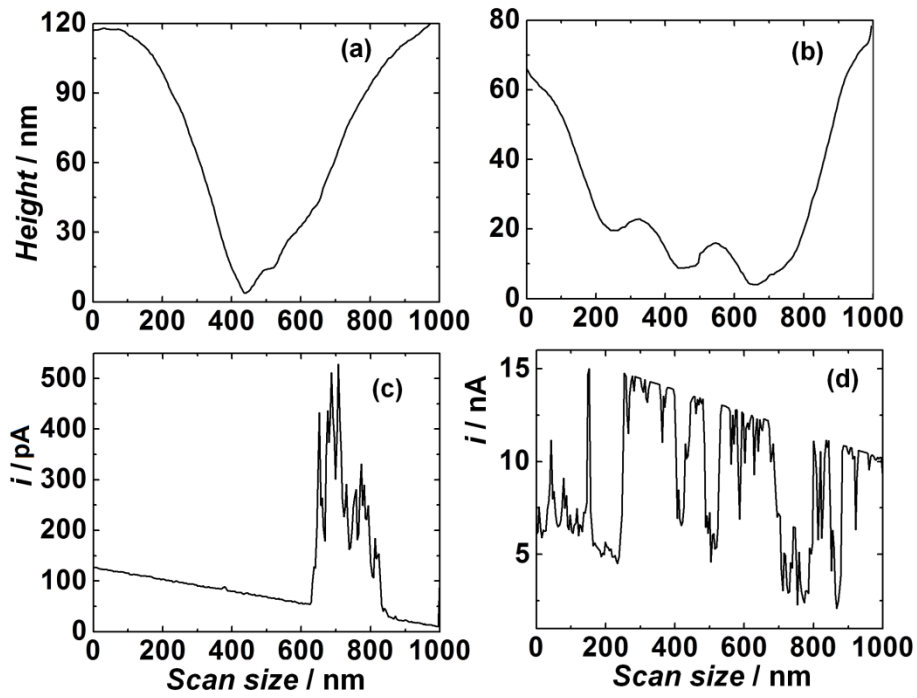


Figure S4 Cross-sectional profiles of topography (a,b) and current (c,d) images of PCIND and PEDOP derived from Figure 2.

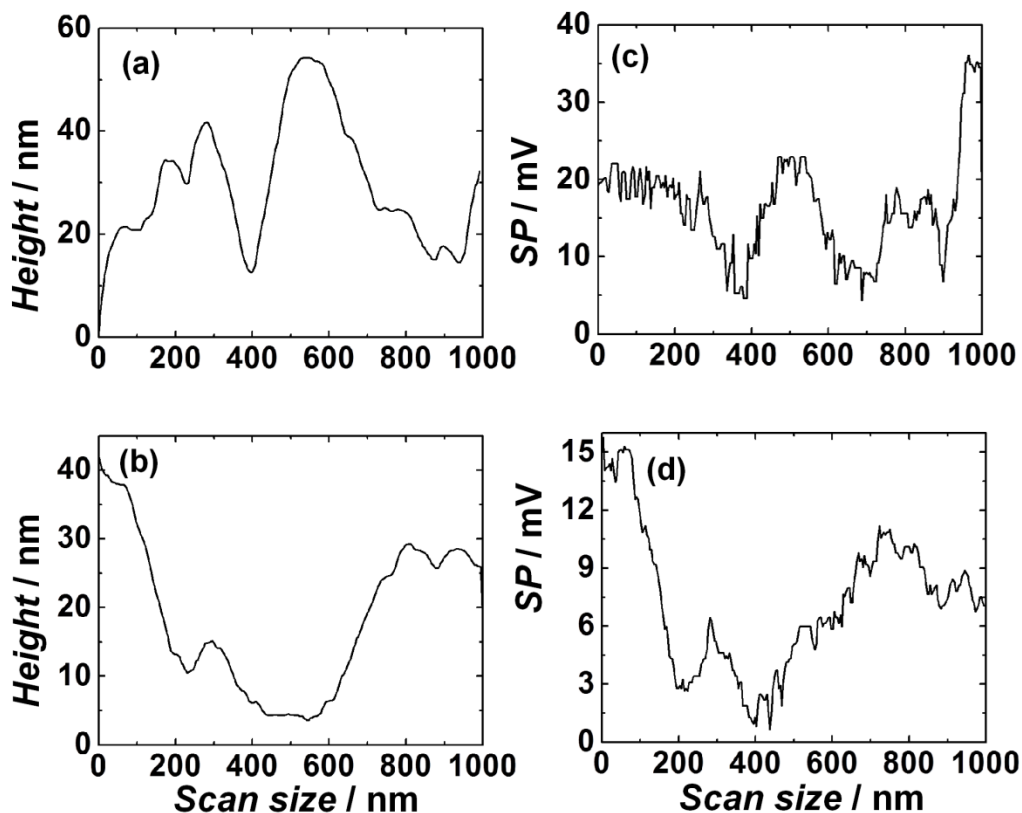


Figure S5 Cross-sectional profiles of topography (a,b) and surface potential (c,d) images of PCIND and PEDOP derived from Figure 3.

Determination of energy level positions (Figure 3):

Conduction band positions of PEDOP and PCIND:

From the cyclic voltammograms of PEDOP and PCIND recorded at a sweep rate of  $2 \text{ mV s}^{-1}$  (Figure 6), the oxidation peaks were observed at potential ( $E_O$ ) of  $0.9 \text{ V}$  (*versus*  $\text{Ag}/\text{Ag}^+$ ) and  $0.4 \text{ V}$  (*versus*  $\text{Ag}/\text{Ag}^+$ ). The potential of reference electrode ( $\text{Ag}/\text{Ag}^+$ ) was  $+0.197 \text{ V}$  (*versus* NHE). The oxidation potential (*versus* NHE) corresponds to the highest occupied molecular orbital (HOMO) position or valence band position of the electroactive material.

Therefore, the oxidation potential of PEDOP (*versus* NHE) will be:  $E_O = (0.6 + 0.197) \text{ V} = 0.797 \text{ V}$ .

The oxidation potential of PCIND (*versus* NHE) will be:  $E_O = 0.9 + 0.197 \text{ V} = 1.097 \text{ V}$ .

0 V (*versus* NHE) corresponds to 4.5 eV (w.r.t. vacuum level). The VB positions of PEDOP and PCIND are therefore 5.297 and 5.597 eV respectively.

Band gaps ( $E_g$ ) of PEDOP and PCIND: The absorption edge wavelengths were obtained by extrapolating the absorption spectra of PEDOP and PCIND (in their red and blue states respectively). Using  $E_g = hc/\lambda$ , where  $c$  is the speed of light, the band gaps of PEDOP and PCIND were 1.82 and 1.41 eV respectively.

Determination of Fermi levels of PEDOP and PCIND from KPFM:

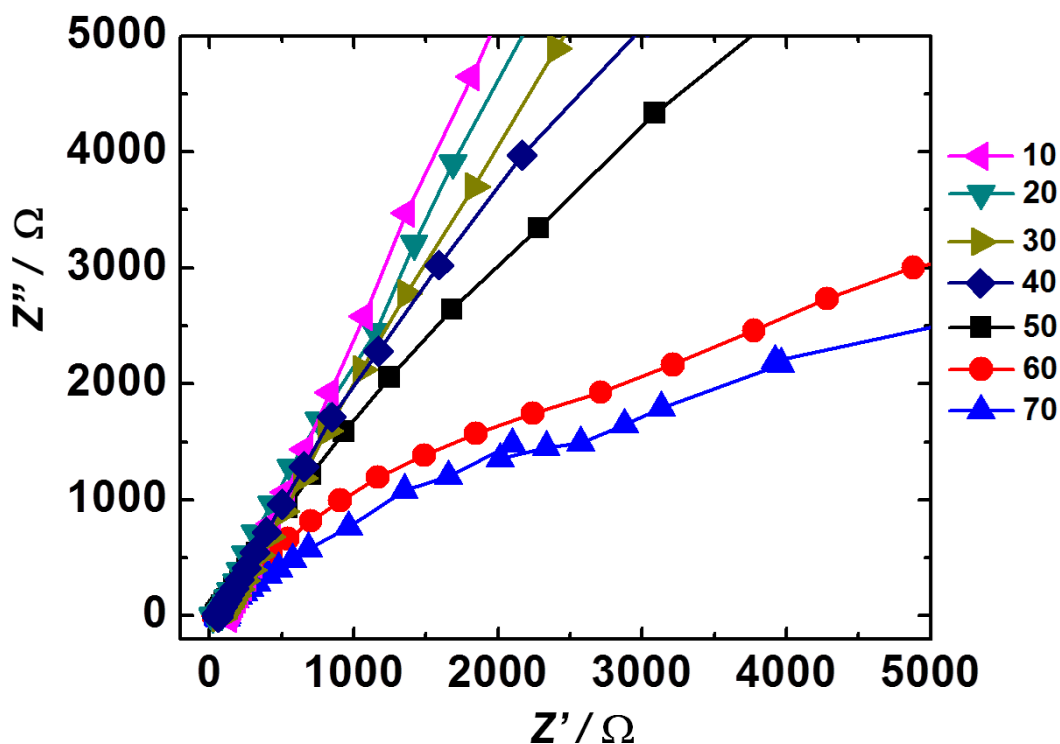


Figure S6  $Z''$  versus  $Z'$  plots for the [BMPY][N(CF<sub>3</sub>SO<sub>2</sub>)<sub>2</sub>]-PVdF-HFP-PC gel electrolyte recorded at different temperatures (in °C, represented by symbols), over a frequency range of 0.1 Hz to 1 M Hz.

Equations used for calculating  $R_e$  and  $R_{ion}$ :

$$1/(R_h - R_s) = 1/R_e + 1/R_{ion} \quad (1)$$

$$3(R_l - R_s) = R_e + R_{ion} \quad (2)$$

$R_s$  is the solution resistance, which can be obtained from the impedance curve generated by using a bare FTO-coated glass substrate as the working electrode. The  $R_h$  is the value that is the high frequency real axis intercept minus  $R_s$ .  $R_l$  is the low frequency limiting real impedance. The  $R_e$  and  $R_{ion}$  are the electronic and ionic resistances of the films. These plots are shown in Figure S7.  $R_e$  and  $R_{ion}$  were determined by solving equations 1 and 2. The  $\sigma$ ,  $R$ ,  $l$  and  $a$  are the conductivity, resistance, thickness and surface area of the films in equations 3 and 4.

$$\sigma_e = l/R_e \times l/a \quad (3)$$

$$\sigma_{ion} = l/R_{ion} \times l/a \quad (4)$$



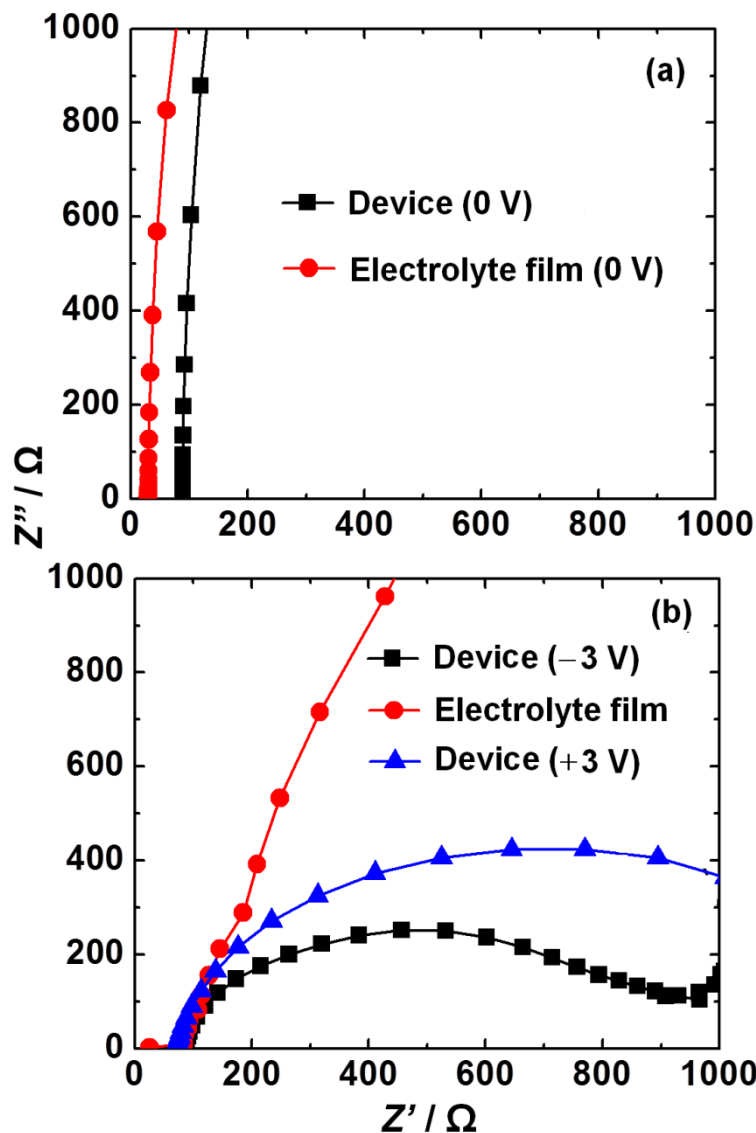


Figure S7 Electrochemical impedance spectra of (a) the [BMPY][N(CF<sub>3</sub>SO<sub>2</sub>)<sub>2</sub>]-PVdF-HFP-PC electrolyte film (●) between two FTO coated glass substrates and the PCIND-[BMPY][N(CF<sub>3</sub>SO<sub>2</sub>)<sub>2</sub>]-PVdF-HFP-PC-PEDOP device (■) recorded under a dc potential of 0 V and (b) for the device under +3 (■) and -3 (▲) V and for the electrolyte between two FTO coated glass substrates under 0 V (●), over a frequency range of 0.1 to 10<sup>6</sup> Hz.

Table S2 EIS parameters for the PCIND-[BMPY][N(CF<sub>3</sub>SO<sub>2</sub>)<sub>2</sub>]-PVdF-HFP-PC-PEDOP device, under different potentials. Capacitances were obtained from the fits.

$E$ (V)	$\sigma_e$ (S cm <sup>-1</sup> )	$\sigma_{ion}$ (S cm <sup>-1</sup> )	$C_{dl}$ ( $\mu$ F)	$C_F$ ( $\mu$ F)
0	$0.6 \times 10^{-4}$	$0.6 \times 10^{-6}$	9.82	12.4
+3	$1 \times 10^{-2}$	$1 \times 10^{-3}$	6.68	43.3
-3	$1.5 \times 10^{-3}$	$4 \times 10^{-4}$	10.2	77.2